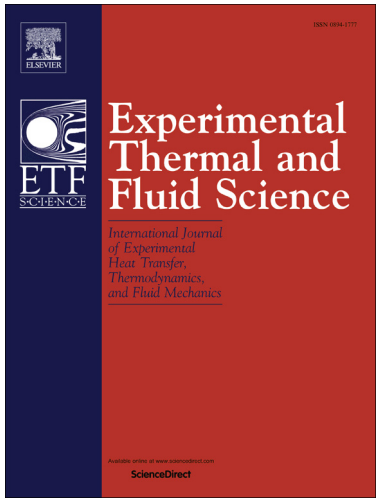

Experimental Investigation of Thermal Performance of Metal Foam Wicked Flat Heat Pipe

D. Somasundaram, A. Mani, M. Kamaraj

PII: S0894-1777(16)30362-4
DOI: http://dx.doi.org/10.1016/j.expthermflusci.2016.12.006
Reference: ETF 8968

To appear in: *Experimental Thermal and Fluid Science*

Received Date: 17 November 2015
Revised Date: 7 December 2016
Accepted Date: 8 December 2016

Please cite this article as: D. Somasundaram, A. Mani, M. Kamaraj, Experimental Investigation of Thermal Performance of Metal Foam Wicked Flat Heat Pipe, *Experimental Thermal and Fluid Science* (2016), doi: http://dx.doi.org/10.1016/j.expthermflusci.2016.12.006

Experimental Investigation of Thermal Performance of Metal Foam Wicked Flat Heat Pipe

D. Somasundaram [a,*], A. Mani [a], M. Kamaraj[b]

[a]Refrigeration and Air-conditioning Laboratory, Department of Mechanical Engineering,

[b] Department of Metallurgical and Materials Engineering,

Indian Institute of Technology Madras, Chennai 600036, India.

Abstract

Experimental investigations of thermal performance of a flat heat pipe (FHP) with and without wick columns were investigated. Copper metal foam fabricated by lost carbonate sintering process and characterized by Scanning Electron Microscope (SEM) was used as wick structure. The effect of heat input, cooling water flow rate, cooling water temperature and fill ratio on the thermal response of the FHP is presented. Results showed that the heat transfer coefficient increases with increased Reynolds number and cooling water temperature but decreases with increased heat input and amount of fill ratio. It was found that increasing the wick volume by inserting additional wick columns improves the FHP performance, due to the decreased thermal resistance with increased fluid movement in these additional wick columns. The experimental results were compared with that of analytical calculations at steady state and a good agreement was observed between them.

Key words: Flat heat pipe; Copper foam; Wick columns (WC); Evaporator; Condenser;

Nomenclature

A	area, m^2
C	specific heat, J/ (kg K)
h	convection heat transfer coefficient, W/ (m^2 K)
H	height of flat heat pipe, m
k	thermal conductivity, W/(m K)
L	length of flat heat pipe, m
Q_e	heat transfer rate, W
Re	Reynolds number ($R_e = \frac{\rho v L}{\mu}$)
R_t	total thermal resistance (^oC/W)
T	temperature, K
V	velocity of fluid, m/s
W	width of flat heat pipe, m
x	axial direction, m
y	height direction, m

Greek symbols

φ	Porosity
μ	Viscosity, Pa s
ρ	Density, kg/m^3
σ	Surface tension, N/m
θ	Wetting angle

Subscripts

a	adiabatic

*Corresponding author: Tel.: +91 44 2257 4666; fax: +91 44 2257 4652

E-mail addresses: soms.iitm@gmail.com, mania@iitm.ac.in, kamaraj@iitm.ac.in,

avg	average	p	pressure
c	condenser	sat	saturation
cw	cooling water	s	solid (wall material)
e	evaporator	v	vapor
eff	effective	w	wick
f	fluid		

1. Introduction

Use of flat heat pipes (FHP) becomes very attractive due to their potential benefits and applications in electric and electronic cooling management. Light weight and compact shape, high heat transport rate with minimal temperature drop and temperature flattening capability are the exclusive features of FHP. These features have motivated many researchers to carry out experimental and numerical investigation on FHP to analyze its thermal performance with various wick structure and working fluid. Due to high latent heat of vaporization and other desirable properties, water has widely been used as a working fluid in these devices. Engineer's and scientist's made great effort to improve wick structure to enhance the heat transfer limitation of the FHP. Porous wicks with porosity between 0.3 and 0.6 have been studied for many decades and an excellent review of those studies has been summarized in Kaviany [1]. William and Harris [2] developed a test apparatus and a technique to determine the heat transfer limit of a planar heat pipe wick. In this technique effective thermal conductivity of the wick was determined and was found to be compatible for many of the low temperature heat pipe working fluids such as water or methanol. To enhance evaporation process, Xuan *et al.* [3]applied a layer of sintered copper powder to the heated surface of the heat pipe. Performance was experimentally measured under different heat fluxes in order to investigate the effects of charge amount of the working fluid, thickness of the sintered layer and the orientation of the heat pipe.

Thermal resistance across the evaporator and condenser section in a FHP is an important parameter to estimate its performance. Hsieh *et al.* [4] carried out experiments to test the thermal resistance of the vapor chamber of FHP used in electronic cooling. It was found that when the applied heat power increases, the evaporation and condensation heat transfer coefficients are increased. Wang and Vafai [5,6]found that the porous wick of the evaporator section forms the main resistance to the thermal flow, resulting in the largest temperature drop. Chang *et al.*[7] investigated the thermal performance of the FHP cooling system by thermal resistance model approach and found that the evaporation resistance and the condensation resistance grow with increased heating power and with decreased fill ratio. The visualization and measurement of evaporation resistance for operating flat plate heat pipes with sintered multi-layer copper mesh wick for different mesh composition, wick thickness, fluid charges and heat loads are measured by Liou *et al.* [8]. The effect of filling ratio, heat fluxes and vapor space thickness of FHP on the liquid distribution and its performance are experimentally studied by Lips *et al.* [9].

A small vapor space thickness induces the liquid retention and thus reduces the thermal resistance of the system but at the same time it reduces the maximum capillary pressure by means of influencing the meniscus curvature radii in the grooves. Boukhanouf *et al.* [10] used infra-red thermal imaging camera to measure temperature distribution on the evaporator surface during steady and transient operation of FHP. Using infrared thermography Wong *et al.* [11] found that overall thermal resistance of the vapor chamber heat sink was declined with increased Reynolds number. At a low Reynolds number, a suitable number of fins can be chosen to ensure favorable thermal performance of the vapor chamber. However, at a high Reynolds number, the thermal performance improves with increase in fin number. With the same length of condensation section, when the evaporation section length was increased, the thermal resistance of FHP was decreased. However the heat transfer limit was found to be increased.

For the same length of evaporation section when the condensation section was increased, the FHP would be dried out but the heat transfer limit is reduced resulting in decrease in evaporator temperature [12]. It was observed that the evaporation resistance was smaller when the wick contains fine powders. Under large heat loads, fine pores at the bottom wick have helped sustain a thin water film by which smaller evaporation resistance as well as large critical loads could be achieved. Singh *et al.* [13] investigated the sintered porous heat sink experimentally for the cooling of the high-powered compact microprocessor for server applications.

Lot of work has been carried out to study the thermal performance of FHP with sintered wick structure. However, high porosity metal foam with porosity in the range of 0.7 is relatively a new development. Metal foam owing to its high heat transfer surface area, open porosity and high permeability is considered to be potentially beneficial of being used for heat sinks. Bhattacharya *et al.* [14] concluded that the effective thermal conductivity strongly depends on porosity and the permeability increases with pore diameter and porosity but inertial coefficient depended on only porosity. The use of the open-cell metal foams in heat transfer application needs an effort to know the behavior of the fluid flowing through its matrix composition and the heat transfer process occurring in the medium. Boomsma and Poulikakos [15] investigated hydraulic performance of open cell metal foam using water as the flow medium. It was found that the permeability and form coefficient are influenced by flow rate. The contribution of inertial and viscous effects for several foam samples with different characteristic of copper and nickel foam is studied by Topin and his co-workers [16].By using powder metallurgy technique copper foam with porosities in the range of 50-85% and cell sizes in the range of 53-1500 μm has been fabricated [17-19]. In order to reduce the adverse effect on the strength of sintered porous metals, binder should be removed completely and by factorial design of experiment it was found that the amount of filler material is the most important parameter for controlling the porosity in the copper foam [20].

As metal foam enhances the fluid flow due to presence of very small pores in the foam's microstructure and a higher permeability than sintered powders, they are preferred as wick structure in FHPs. Metal foam wicked heat pipes are able to manage more heat in any orientation. The temperature distribution of FHP sandwich structure has been investigated both experimentally and computationally [21]. In this analysis, nickel metal foam is used as wick structure and distilled water is used as the working fluid. To assess the thermal management characteristics of FHP using open cell nickel foam, Carbajal *et al.* [22] designed a multifunctional sandwich panel combining efficient structural load and carried out an experimental investigation.

Any existing wicked heat pipe technology can be considerably improved with new wick structures, materials, designs etc., in order to face new challenges in electrical and electronics cooling. The research work carried out on metal foam wicked FHP available in the literature was scanty. In the present experimental investigation, copper metal foam was used as the wick structure for enhanced heat transfer with an objective to move the heat transfer limit of the wicked FHP to a newer height. As the effective thermal conductivity of porous structure is important for low thermal resistance, an optimal balance was achieved between the properties such as porosity and permeability related to fluid flow and heat transfer rate. Different number of wick columns will be tested to study its influence on FHP's thermal performance and comparison will be made on FHP without wick columns. Analytical calculations were performed based on energy balance studies, to estimate the theoretical performance of the FHP and the experimental results were compared.

2. Details of the Experimental Setup

Figure 1 shows the schematic of the experimental flat heat pipe (FHP) system consisting of experimental section, data acquisition system and chiller, evacuation, charging and heating units. The experimental section consists of the FHP and the heater. The FHP was fabricated from copper plates and sealed perfectly to avoid any leakage of the working fluid and to maintain the low pressure inside it. The low pressure was needed inside the FHP to lower the boiling point of the working fluid. The low pressure was produced by a vacuum pump connected to the FHP. A fluid charging unit to supply distilled water was connected to the vacuum pump line in order to facilitate injection of working fluid at appropriate moment. Valves are provided one each in the vacuum pump line and one in the fluid charging line. Another valve close to the FHP was used to isolate the experimental section from the ambient. A pressure gauge was provided in the FHP to monitor the low pressure in the system.

The cooling water enters the test section, which houses the heat pipe frame and the heat pipe and takes away the heat by convection heat transfer. The cooling water pressure and flow rate are stabilized by

the chiller unit. Peristaltic pump was used for the cooling water supply to ensure undisturbed uniform flow to the condensing section. The cooling water flow rate was measured and varied by varying the pump speed.

The heater was provided with electrical heaters and was supplied with power from a power supply unit. A voltage regulator was used to control the power input in order to vary the heat input to the evaporator section. The heating unit consists of a copper block with rod shaped or cylindrical electrical heaters. To obtain a high heat flux, high density rod heater was used in the copper block heating unit. High thermal conductivity cement was used in the gaps between the copper rod and the copper block, to reduce heat loss. In order to reduce contact resistance between the heater block and the FHP, high conductivity grease was applied between their surfaces of contact. The contact between the copper heating block and the FHP was improved with the help of tightening screws provided on the copper block.

Figure 2(a) shows the isometric view of the FHP containing wick columns which are used to increase the fluid flow to the evaporator in addition to the side wicks adjacent to the walls made of copper plates. The space between the wicks inside the FHP forms the vapour core. The dimensions of the FHP presently studied was100 mm in length (L), 100 mm in width (W) and 35 mm in height (H). The FHP wall was 4 mm thick (t_s) and the copper foam wick thickness (t_w) was 2 mm. In the vapor core also, wick column thickness was 2 mm. The calculated wick capillary limits were 802.2 W, 1604.5 W and 2406.5 W for no WC, 1 WC and 2 WC respectively. Heat was supplied (Q_e) by a heater placed on the top surface of FHP's evaporating section. The heating unit covers the length of the FHP and has a width of L_e. The condenser section of the FHP was covering the entire bottom surface of the FHP. The heat from the FHP was rejected to the cooling water circulated in the bottom.

Figure 2(b) shows the cross sectional view of FHP with the heater, cooling jacket and the ceramic blanket which was used to insulate the heat pipe kept inside a sheet metal box. Wicks are found attached to the top and bottom plates of the FHP. The heater was placed above the top plate and cooling water channel was provided below the bottom plate. The entire assembly was insulated from outside to prevent thermal loss to the ambient.

The temperatures are measured by T-type thermocouples and collected through a data acquisition system. The precision of the T-type thermocouples in the present work is found to be 0.5 C. Twenty two locations of thermocouples along the width of the FHP, that are used to measure the temperature distribution on the evaporator and condenser surface are shown in Figure 2(c). In order to monitor the heat loss through the insulated surfaces, thermocouples are also fixed on both the inner and outer surfaces of the FHP cover box. In addition, two thermocouples are incorporated to monitor the cooling water temperature at the inlet and outlet, and one thermocouple is placed outside to measure the room temperature. The thicknesses of top

and bottom plates of the FHP are 4 mm which enables insertion of the thermocouples. The holes for inserting the thermocouples are 2 mm in depth and 1 mm in width. To reduce the contact resistance and the temperature measurement error, high conductivity grease is applied into these holes. The distance between adjacent thermocouple on the evaporator and condenser region was 9 mm.

Raw materials used for manufacturing copper foam are pure copper powder and potassium carbonate in powder form. Energy dispersive X- ray (EDX) analysis is carried out to determine the purity of the copper powder and potassium carbonate. The size of the filer material is selected based on intended pore diameter of the metal foam. The copper powder contains spherical particles. The potassium carbonate powder has spherical granular particles. Both the powders are mixed based on the desired porosity of the metal foam. The particle size of the copper powder is not critical, but the particle diameter is smaller than that of potassium carbonate particles. Ethanol is used as binder to ensure both the powders are mixed uniformly. The percentage of adding ethanol to the mixture is small and estimated roughly 1.5% of volume of mixtures. Physical properties of a copper foam wick like average porosity and pore radius, as given in Table 1, are measured by image analyzing techniques [23]. SEM micrographs of details of the copper powder, filler material, sample foam structure and pore and its walls are presented in Fig. 3 at different magnification scales that show the distribution of uniform pores fused together at the interfaces.

3. Experimental Procedure

Distilled water was used as the working fluid. The vacuum pump was used to bring the heat pipe to vacuum condition and the working fluid was injected into it, by operating appropriate valves, as shown in Fig 1. The valve connecting the vacuum pump and the FHP was closed before opening the fluid charging line valve to avoid fluid getting sucked into the vacuum pump. When the fluid charging unit valve was opened, the fluid gets sucked in to the FHP due to the low pressure prevailing in it. Due to this low pressure, there exists a possibility for part of the water injected to get evaporated. After injecting distilled water, the heat pipe is vacuumized again. But this time, the heat pipe was heated during the vacuumizing process in order to extract as much residual air as possible and also to produce water vapour. This will ensure that the heat pipe is full of vapor of the working fluid and later the FHP was sealed. The sealed heat pipe was kept in room conditions for 24 hours and the heat pipe pressure was monitored by a vacuum gauge connected to it, for any possible leakage. The heat pipes that show a stable gauge pressure for the entire period only were used for conducting experiments.

The liquid boils at the evaporation surface with the heat supplied and the vapor flows down and condenses on the condensation surface. In this way the heat can be transferred from the evaporator to the condenser. The evaporation of distilled water in the wick at the evaporator surface causes the wick to get

dried up. This generates a driving potential for the water in the FHP bottom to rise up through the vertical wick columns against gravity.

In this study, heat input, cooling water flow rate, cooling water temperature and amount of working fluid are varied. In each experimental run, only one parameter is varied at a time and others are maintained constant. For a typical experimental run, heat input to the evaporator is varied for a fixed amount of working fluid after reaching a steady flow rate at a constant cooling water temperature. The measured parameters include temperatures on the heat pipe surfaces, the temperature of the cooling water at inlet and outlet, the flow rate, and the input power. The temperatures at all the locations are sampled every 10 second and are collected through the data acquisition system. The power supply is turned off when steady-state condition is achieved. The steady-state conditions is assumed to be reached when the changes of the maximum temperature reading is less than 0.5°C for a minimum period of 5 minutes.

3. Data reduction

Temperature gradients are estimated only after the steady state temperature distribution is obtained. The heat flux of the heating unit is deduced from Fourier's law of heat conduction. An average of cooling water temperature and condenser temperature is considered as the film temperature. For applied power input, cooling water temperature, cooling water flow rate and fill ratio, heat transfer coefficient is calculated on the basis of film temperature. Heat transfer coefficient, total thermal resistance of FHP and temperature drop across the heat pipe can be calculated by the following expressions at each experimental run.

The heat transfer rate on the condenser side wall to the cooling water Q_c is estimated as

$$Q_c = h_c A_c (T_c - T_{cw}) \tag{1}$$

where h_c is the condenser side convection heat transfer coefficient, A_c is the condenser surface area, T_c is the condenser surface temperature and T_{cw} is the cooling water inlet temperature.

The thermal resistance between the evaporator and condenser for the given evaporator heat input is given as,

$$R_t = \frac{(T_e - T_c)}{Q_e} \tag{2}$$

$$T_{w,c} = T_c + \frac{(Q_e t_c)}{(A_c k_s)} \tag{3}$$

$$T_{w,c,v} = T_{w,c} + \frac{(Q_e t_w)}{(A_c k_{eff})} \tag{4}$$

$$T_{w,e} = T_e - \frac{(Q_e t_c)}{(A_e k_s)} \tag{5}$$

$$T_{w,e,v} = T_{w,e} - \frac{(Q_e t_w)}{(A_e k_{eff})} \tag{6}$$

$$T_v = \frac{(T_{w,c,v} + T_{w,e,v})}{2} \tag{7}$$

The effective thermal conductivity of metal foam can be found from the correlation developed by Bhattacharya *et al.*[14] which is given below.

$$k_{eff} = 0.35\left[\varphi k_f + (1-\varphi)k_s\right] + 0.65\left(\frac{\varphi}{k_f} + \frac{1-\varphi}{k_s}\right)^{-1} \tag{8}$$

4. Uncertainty analysis

A computer based data acquisition system was used to record the measurements from all these instruments and sensors continuously. Calibrated instruments are used to measure temperature and flow rate. Uncertainty estimates are carried out by considering the errors of the instruments, the measurement variance, geometry uncertainty and calibrations errors for the heat flux and temperature measurements. Uncertainties in the measured quantities namely heat input, temperature, pressure, and flow rates are determined from the minimum value of the measured output and accuracy of the instruments [24]. The measurement uncertainties of copper constantan thermocouples are estimated to be ± 0.5 ^{o}C and that of pressure gauges is ± 2.6%. Substrate conduction heat losses are quantified at different power inputs. The primary contributor to heat flux uncertainty is the heated surface area. Combining these effects contributes to overall uncertainty estimates in heat flux of 7% at the average heat input. Based on these values, the uncertainty of the heat transfer coefficient is found to be about ±9.5%.

4. Results and Discussions

4.1. Effect of Heat Input

Figure 4shows excellent agreement between the experimental and the analytical condenser surface temperature for different heat input, cooling water flow rate, cooling water temperature and working fluid charge. It is found that the measured condenser surface temperatures are a little lower than the analytical temperatures under steady-state conditions. Due to three dimensional heat transfers along the top wall, the large amount of heat is transferred in the normal direction from the evaporator section to the condenser section through the evaporation and condensation process. The top wall also provides a secondary conduction path for the heat flow in the longitudinal direction which is not considered in the analytical

model. Based on the heat conduction model, analytical study accounts the input heat transfer rate, cooling water temperature, convective heat transfer coefficient from the experimental study and geometrical properties of FHP and copper wick and thermo physical properties of water [25-28].

Figure 5 shows the effect of wick columns on the temperature rise for the evaporator and condenser surface of the heat pipe for different heat input while the cooling water temperature and flow rate are kept constant. As expected, the evaporator as well as condenser surface temperature increases with an increase in heat input. However, increasing heat input has less effect on average surface temperature rise of both evaporator and condenser with increasing number of wick columns (WC) since wick columns increase the mass flow rate of the liquid to the evaporator section. Figure 6 shows the thermal resistance of FHP for different heat input. As illustrated, thermal resistance of FHP is decreased when the numbers of wick columns are increased. As a result, for the same heat input, the temperature difference of evaporator and condenser is decreased due to addition of wick columns.

Figure 7 shows the effect of addition of wick columns on heat transfer coefficients for different heat fluxes. Increasing heat input has significant effect on the condenser surface temperature. If the heat input increases, the condenser surface temperature also increases. Heat transfer coefficient is a function of condenser surface temperature when the cooling water temperature is kept constant for the desired flow rate. As a result, for increased heat input, heat transfer coefficient is decreased. For the FHP with wick columns, heat transfer coefficients are further decreased due to decrease in condenser surface temperature. Fig.8. shows the effect of heat input on the vapor temperature of FHP during steady stat operation of FHP. As the heat input increases, the vapor temperature also increases. The similar trend is followed for heat pipe with one and two wick columns.

4.2. Effect of Cooling Water Flow Rate

The effect of cooling water flow rate on the average surface temperature of condenser and evaporator can be seen in Fig. 9 for the constant heat flux and cooling water temperature. As shown, increasing the flow rate reduces the evaporator and condenser surface temperature of FHP. With addition of wick columns, the average surface temperature sure is decreased further. When number of wick columns is increased, as expected the average surface temperature is also decreased due to more liquid return. An increasing flow rate increases thermal resistance of FHP for a fixed input power as shown in Fig.10. It is found that the increase in flow rate has insignificant effect on the thermal resistance of FHP even though additional wick columns enhance the liquid return mechanisms. Figure 11 shows the significance of Reynolds number on the heat transfer coefficient of condenser surface for constant heat input at fixed cooling water temperature. It is observed that heat transfer coefficient is increased when the flow rate is increased. Increasing flow rate is also associated with high heat transfer rate. As a result of more condensation, the condenser surface

temperature is decreased. Due to addition of wick columns, the heat transfer coefficient is reduced for the same flow rate. It is due to reduction in condenser temperature of FHP. Figure 12 shows the significance effect of cooling water flow rate on the vapor temperature. As the flow rate increases, the vapor temperature decreases for same heat input at fixed cooling water temperature. At particular flow rate, the vapor temperature is more for FHP with two wick columns due to more vapor formation.

4.3. Effect of Cooling Water Temperature

The effect of cooling water temperature on the surface temperature of condenser and evaporator are plotted in the Fig. 13 when the flow rate is kept constant for constant input heat flux. As shown, when the cooling water temperature increases, surface temperature on both condenser and evaporator increases. For FHP with wick columns, the surface temperature of evaporator increases and condenser temperature decreases at desired cooling water temperature. Due to fluid return mechanism, the condenser temperature is reduced. Figure 14 shows the significance of increasing cooling water temperature on the thermal performance of FHP. As expected the thermal resistance is increased with increased cooling water temperature. But due to addition of wick columns, the temperature difference of the condenser and evaporator is reduced. As a result, the thermal resistance of FHP is significantly reduced at desired cooling water temperature. The wicks in the evaporator and condenser section contribute the largest resistance to the total heat transfer. Due to uniform pore distribution on condenser and evaporator wick, the liquid is spread across the wick uniformly. Figure 15 shows that an increase in cooling water temperature results in increases in the heat transfer coefficient for constant heat input. However, addition of wick columns within the heat pipe is sensitive to the changes in the heat transfer coefficient. The number of wick columns rise refers to the decrease in the heat transfer coefficient of the FHP. Figure 16 illustrates the importance of cooling water temperature of the operating temperature of FHP. As expected, the vapor temperature increases with increased cooling water temperature for constant heat input at particular cooling water flow rate. Vapor temperature with two wick columns is higher than that of heat pipe with no wick column.

4.4. Effect of Fill Ratio

Figures 17 to 20 show the effect of fill ratio on the surface temperature, thermal resistance, heat transfer coefficient and vapor temperature of FHP for constant heat input when the cooling water flow rate and temperature are maintained constant. As can be seen in Fig. 13 evaporator surface temperature decreases and condenser surface temperature increases slightly with increases in fluid charge into the heat pipe. For the FHP with wick columns, the same trend is followed. But the difference in temperature of evaporator and condenser surface is reduced when the number of wick columns is increased. As a result the thermal resistance of FHP is decreased when the fluid charge is increased as shown in Fig. 15.Figure 16 displays effect of fill ratio within the heat pipe as a function of the heat transfer coefficient. When the fill ratio is increased, the temperature of the condenser is decreased. Consequently the temperature difference between

condenser surface and cooling water temperature is increased and resulted in decreased heat transfer coefficient. The increase of introduction of wick column further increases the temperature difference and results in further decreases of heat transfer coefficient. Figure 20 shows the insignificant effect of fill ratio on the vapor temperature of FHP. But for the same working fluid charge, vapor temperature is higher than that of FHP with one wick column and with no wick column.

5. Conclusions

1. The increase in heat input, increases average surface temperature, vapor temperature and thermal resistance of the heat pipe whereas it decreases the heat transfer coefficient.
2. For a specific heat input, the increase in number of wick columns reduces the thermal resistance of the FHP studied. For varied heat input, addition of one wick column decreases the thermal resistance by 1.7-2.1%. Whereas addition of two wick columns, decreases the thermal resistance by 2.4-3.2%.
3. An increase in R_e, reduces the average surface temperature, vapor temperature where as it increases the heat transfer co-efficient and thermal resistance of the heat pipe. For a specific R_e, increasing wick column decreases the heat transfer coefficient where as it increases the average surface temperature, thermal resistance and vapor temperature. The same trend is followed for all the values of Re.
4. The increase in cooling water temperature increases all the parameters studied. For specific cooling water temperature, the increasing wick column, increases average surface temperature and vapor temperature where as it decreases heat transfer coefficient and thermal resistance.
5. The increase in fill ratio decreases all the parameters studied. For specific working fluid charge, the increasing wick columns, increases average surface temperature and vapor temperature where as it decreases heat transfer coefficient and thermal resistance.

References

[1] M. Kaviany, Principles of Heat Transfer in Porous Media, Second Edition, Springer-Verlag, New York, 1995.
[2] R.R. Williams, D. K. Harris, A device and technique to measure the heat transfer limit of a planar heat pipe wick, Exp. Therm. Fluid Sci. 30 (2006) 277–284.
[3] Y. Xuan, Y. Hong, Q. Li, Investigation on transient behaviors of flat plate heat pipes, Exp. Therm. Fluid Sci. 28 (2004) 249–255.
[4] S. S. Hsieh, R. Y. Lee, J. C. Shyu, S. W. Chen, Thermal performance of flat vapor chamber heat spreader, Energy Convers. Manage. 49 (2008) 1774–1784.
[5] Y. Wang, K. Vafai, An experimental investigation of transient characteristics on flat - plate heat pipe during start up and shutdown operations, J. Heat Transfer 122 (2000) 525-535.
[6] Y. Wang, K. Vafai, An experimental investigation of the thermal performance of an asymmetrical flat plate heat pipe, Int. J. Heat Mass Transfer 43 (2000) 2657-2668.
[7] Y. W. Chang, C. H. Cheng, J. C. Wang, S. L. Chen, Heat pipe for cooling of electronic equipment, Energy Convers. Manage. 49 (2008) 3398–3404.
[8] J. H. Liou, C. W. Chang, C. Chao, S. C. Wong, Visualization and thermal resistance measurement for the sintered mesh wick evaporator in operating flat-plate heat pipes, Int. J. Heat Mass Transfer 53 (2010) 1498–1506.
[9] S. Lips, F. Lefèvre, J. Bonjour, Combined effects of the filling ratio and the vapour space thickness on the performance of a flat plate heat pipe, Int. J. Heat Mass Transfer 53 (2010) 694–702.
[10] R. Boukhanouf, A. Haddad , M. T. North, C. Buffone, Experimental Investigation of flat plate heat pipe performance using IR thermal imaging camera, Appl. Therm. Eng. 26 (2006) 2148-2156.
[11] S. C. Wong, Y. C. Lin, J. H. Liou, Visualization and evaporator resistance measurement in heat pipes charged with water, methanol or acetone, Int. J. Therm. Sci. 52 (2012) 154-160.
[12] S. C. Wong, Y. C. Lin, Effect of copper surface wettability on the evaporation performance: Tests in a flat-plate heat pipe with visualization, Int. J. Heat Mass Transfer.54 (2011) 3921–3926.
[13] R. Singh, A. Akbarzadeh, M. Mochizuki, Sintered porous heat sink for cooling of high-powered microprocessors for server applications, Int. J. Heat Mass Transfer 52 (2009) 2289–2299.
[14] Bhattacharya, V. V. Calmidi, R. L. Mahajan, Thermo physical properties of high porosity metal foams, Int. J. Heat Mass Transfer. 45 (2002) 1017-1031.
[15] K. Boomsma, D. Poulikakos, The Effects of Compression and Pore Size Variations on the Liquid Flow Characteristics in Metal Foams, J. Fluids Eng, 124 (2002) 263-269.
[16] F. Topin, J. P. Bonnet, B. Madani, L. Tadrist, Experimental Analysis of Multiphase Flow in Metallic foam: Flow Laws, Heat Transfer and Convective Boiling, Adv. Eng. Mat. 8 (2006).
[17] Y. Y. Zhao, T. Fung, L. P. Zhang, F.L. Zhang,Lost carbonate sintering process for manufacturing metal foams, Scripta Materialia, 52 (2005) 295–298.
[18] Y. M. Z. Ahmed, M. I. Riad, A. S. Sayed, M. K. Ahlam , M. E. H. Shalabi, Correlation between factors controlling preparation of porous copper via sintering technique using experimental design, Powder Technology, 175 (2007) 48–54.
[19] Wang, E. Zhang, On the compressive behavior of sintered porous coppers with low-to-medium porosities - Part II: Preparation and microstructure, Int. J. of Mechanical Sciences, 50 (2008) 550–558.
[20] Y.M.Z. Ahmed , M.I. Riad , A.S. Sayed , M.K. Ahlam , M.E.H. Shalabi, Correlation between factors controlling preparation of porous copper via sintering technique using experimental design, Powder Technology 175 (2007) 48–54
[21] G. Carbajal , C. B. Sobhan , G. P. Peterson , D. T. Queheillalt, H. N. G. Wadley, Thermal response of a flat heat pipe sandwich structure to a localized heat flux, Int. J. Heat Mass Transfer 49 (2006) 4070–4081.
[22] G. Carbajal, C. B. Sobhan, G. P. Bud Peterson, D. T. Queheillalt, Haydn N. G. Wadley, A quasi-3D analysis of the thermal performance of a flat heat pipe, Int. J. Heat Mass Transfer 50 (2007) 4286–4296.
[23] D. Somasundaram, A. Mani, M. Kamaraj, Heat and Fluid Flow Characteristics of Copper Metal Foam as Heat Pipe Wick Material, Appl. Mech. and Mater 787 (2015) 112-116.
[24] S. J. Kline, F. A. McClintock, Describing uncertainties in single sample experiment, Mechanical Engineering 75 (1953) 3-8.
[25] J. M. Tournier, M. S. EL-Fenk, A heat pipe transient analysis model, Int. J. Heat Mass Transfer 37

(1994) 753-762.
[26] D. Somasundaram, A. Mani, Experimental studies on porous wick flat plate heat pipe, International Refrigeration and Air Conditioning Conference, Purdue, (2010).
[27] S. W. Chi, Heat pipe theory and Practice, Hemisphere, New York, 1976.
[28] D. A. Reay, P. A. Kew, Heat pipes, Fifth Edition, Butterworth-Heinemann, 2006.

List of Figures:

Table 1.Thermo physical properties of the FHP materials and the working fluid [28]

Material	Parameters	Value
Copper	Thermal conductivity(k_s)	401 W/m k
	Specific heat(C_p)	385 J/kg K
	Density(ρ_s)	8960 kg/m^3
Wick	Porosity(ε)	0.78
	Permeability(K)	1.114e ×10^{-10} m^2
Water	Thermal conductivity(k_f)	0.6435 W/m K
	Specific heat(ρ_l)	4.18 kJ/kg K
	Viscosity(μ_l)	5.47×10^{-4}Pa s
	Density(ρ_l)	988 kg/m^3
	Latent heat (h_{fg})	2382 kJ/kg
Water vapor	Thermal conductivity(k_v)	0.0196 W/m K
	Specific heat(ρ_v)	1.946 kJ/kg K
	Viscosity((μ_v)	1.0616×10^{-5}Pa s
	Density(ρ_v)	Ideal gas

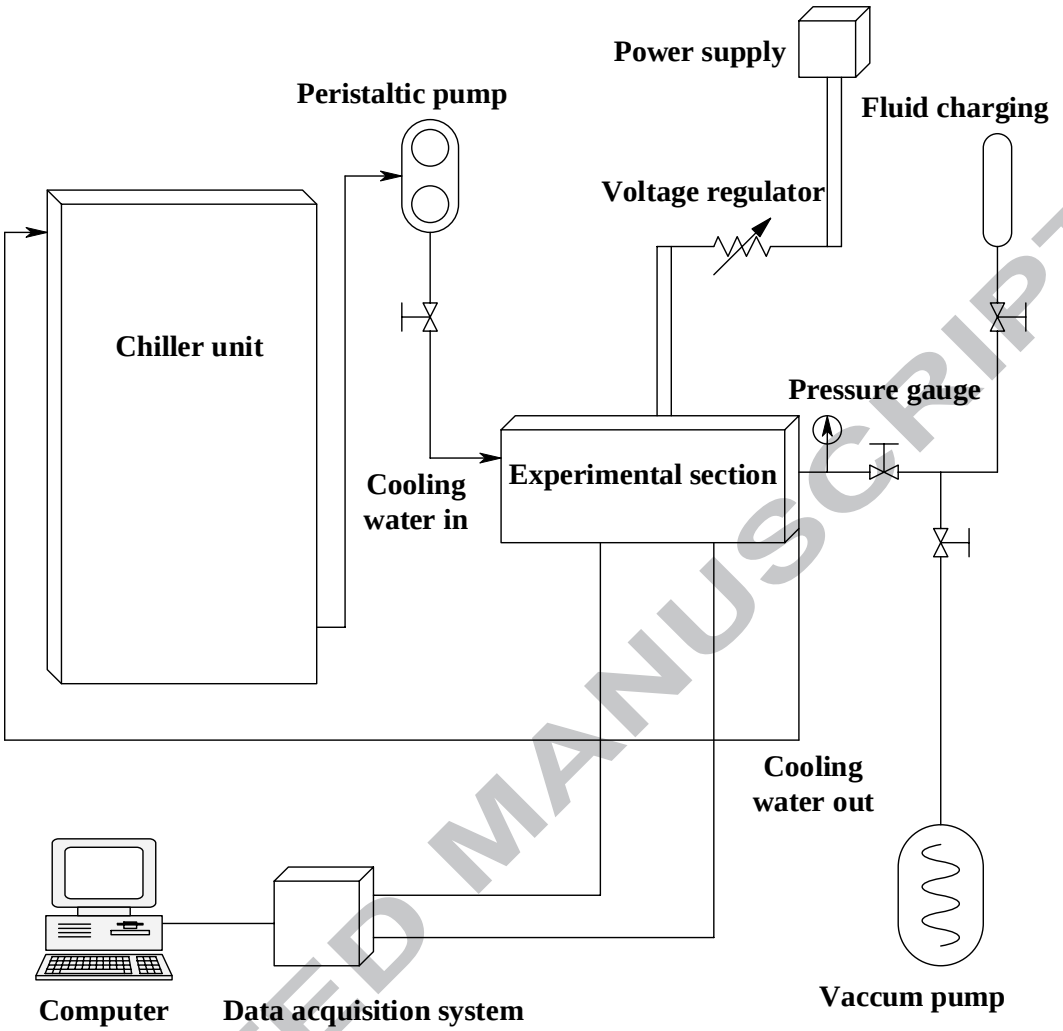

Fig.1 Schematic layout of the FHP experimental set up

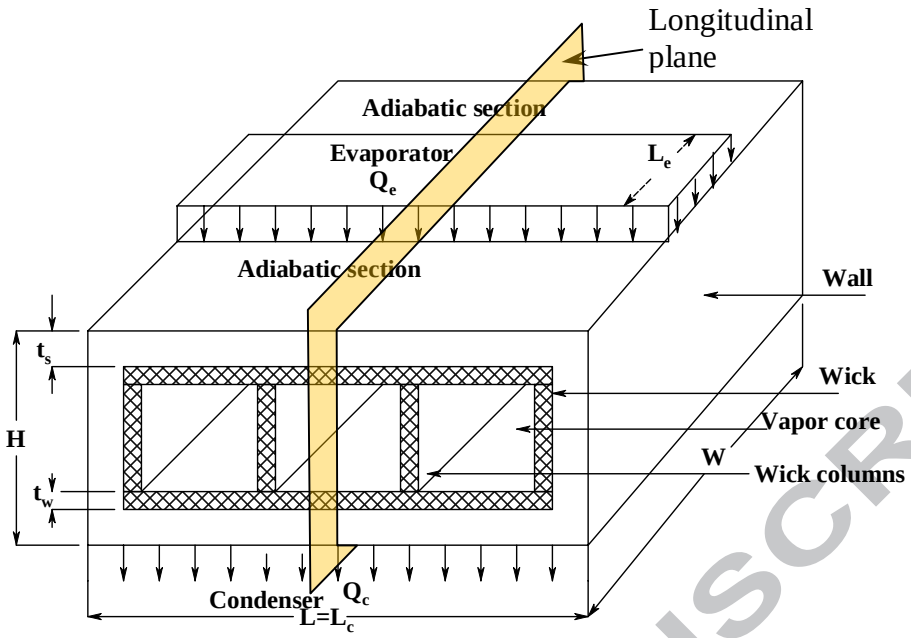

(a) Three dimensional view of the FHP

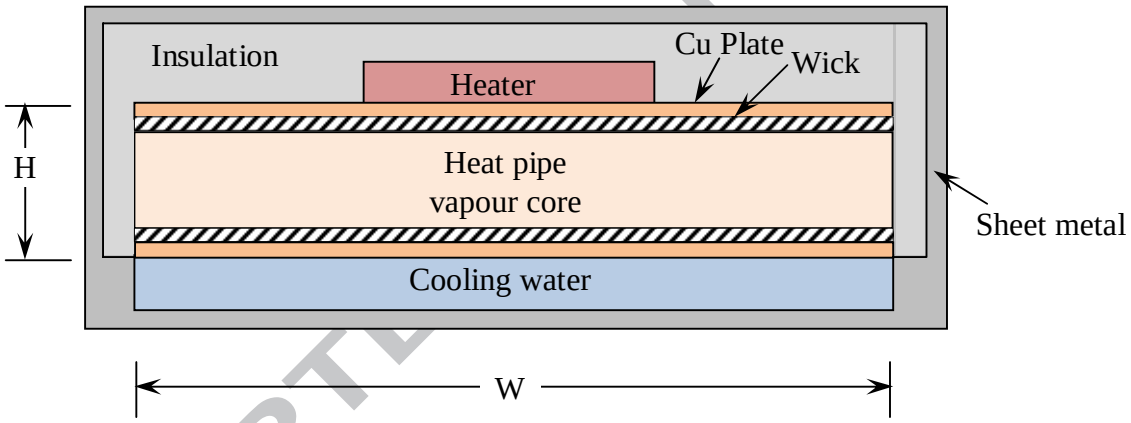

(b) Sectional view of the FHP along the longitudinal plane

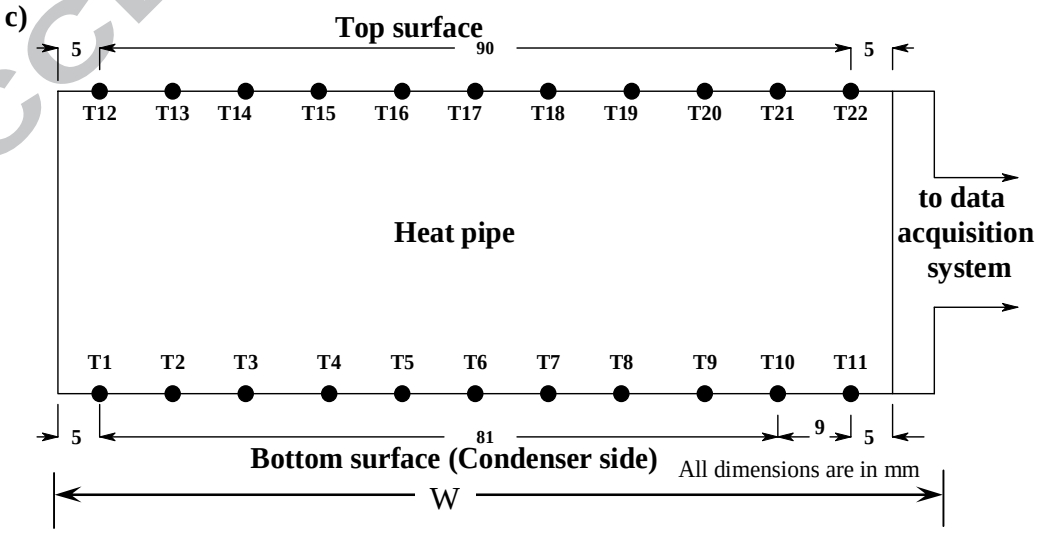

(c) Thermocouple locations on the FHP.

Fig. 2 Details of the FHP with instrumentation

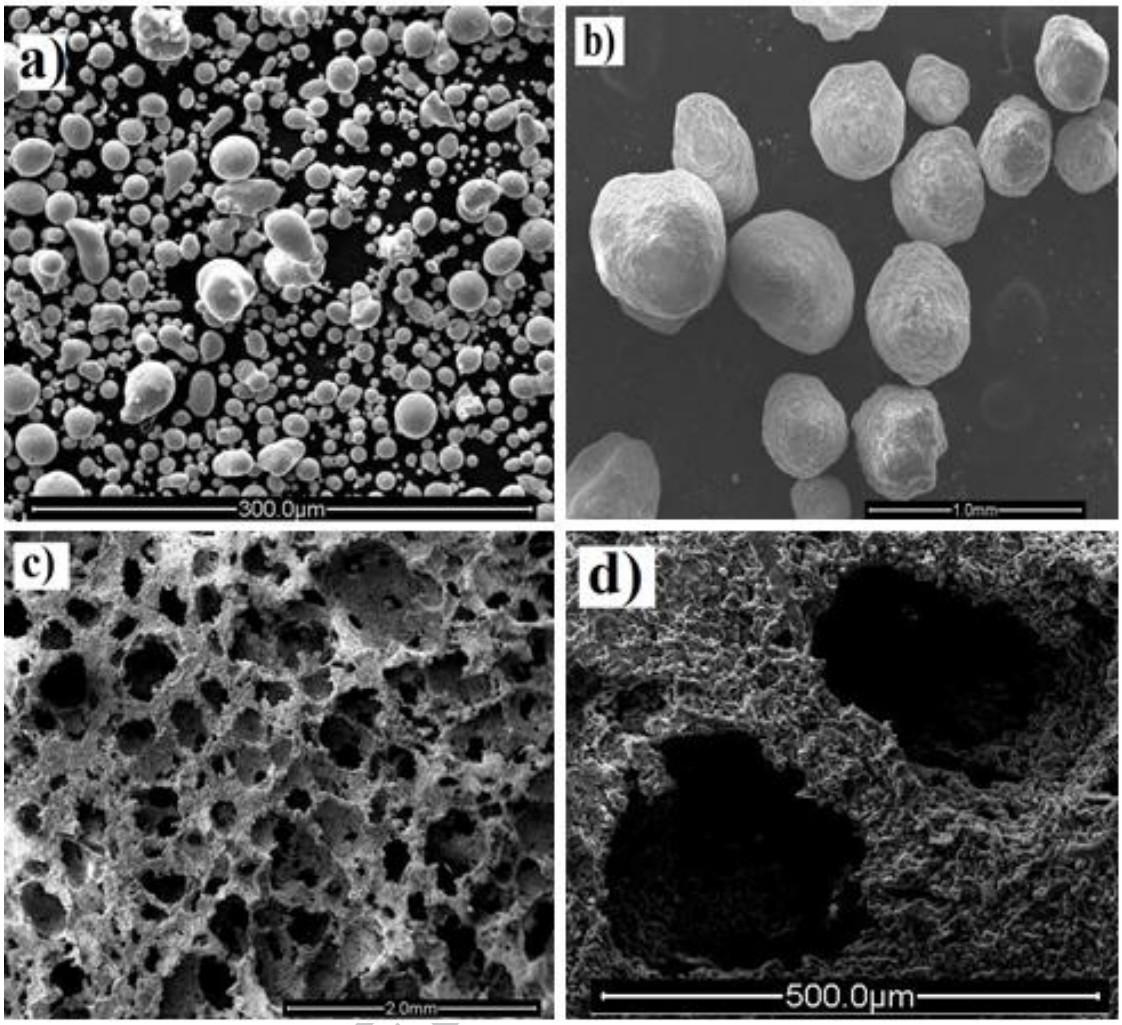

Fig.3. SEM micrographs of particle distribution of
a)Copper powder and b) Pottasium carbonate
c) structure of copper foam and d) pores and its walls

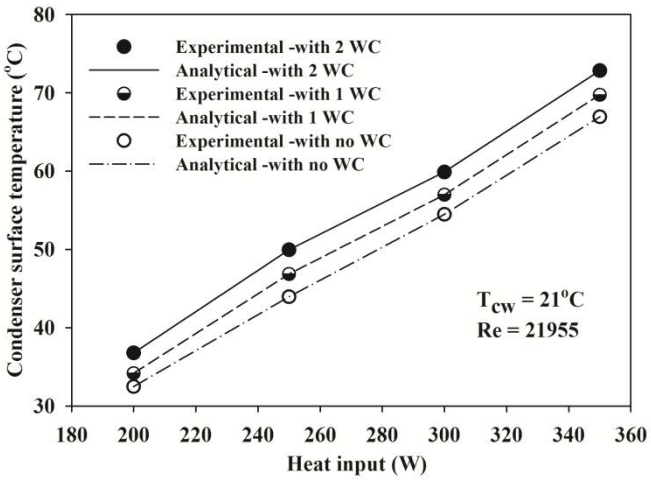

(a)

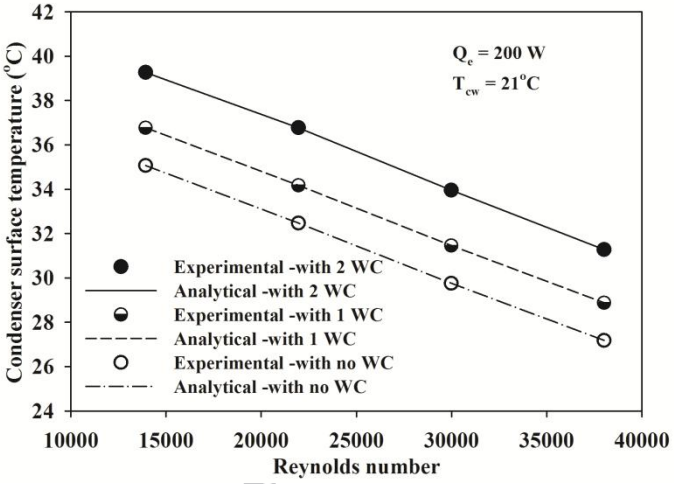

(b)

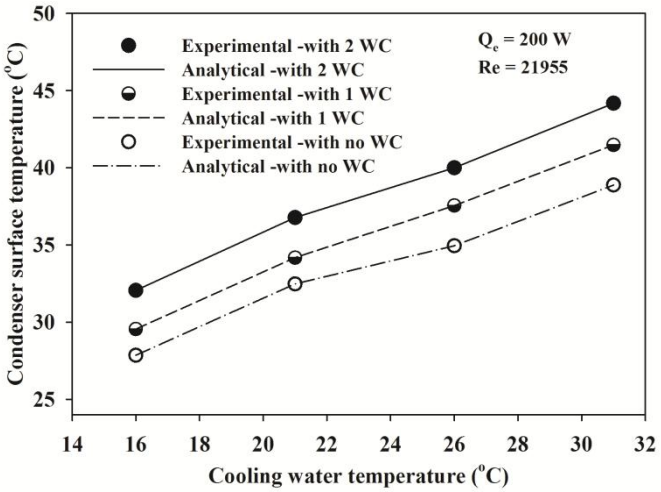

(c)

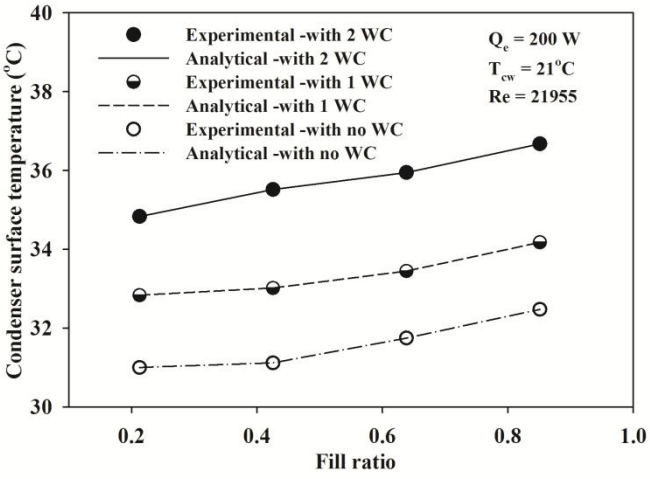

(d)

Fig. 4 Comparison between experimental and analytical model

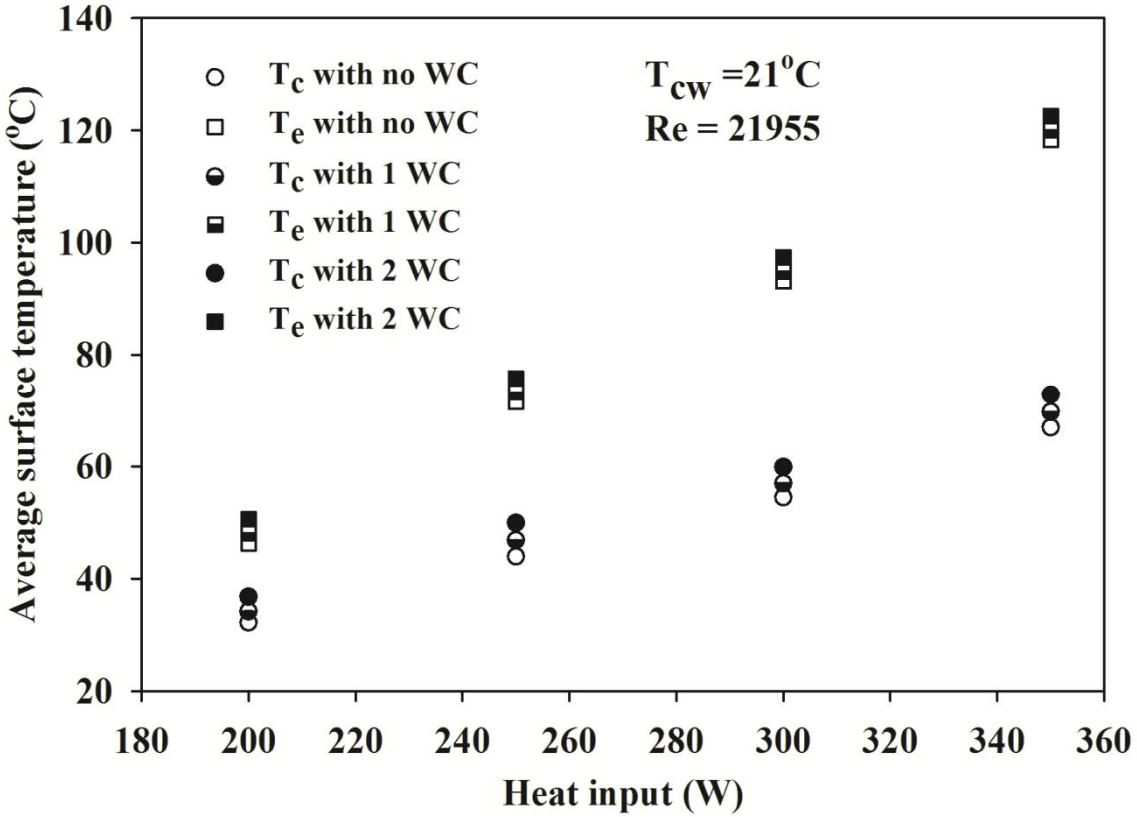

Fig. 5 Effect of heat input on temperature of evaporator and condenser of FHP

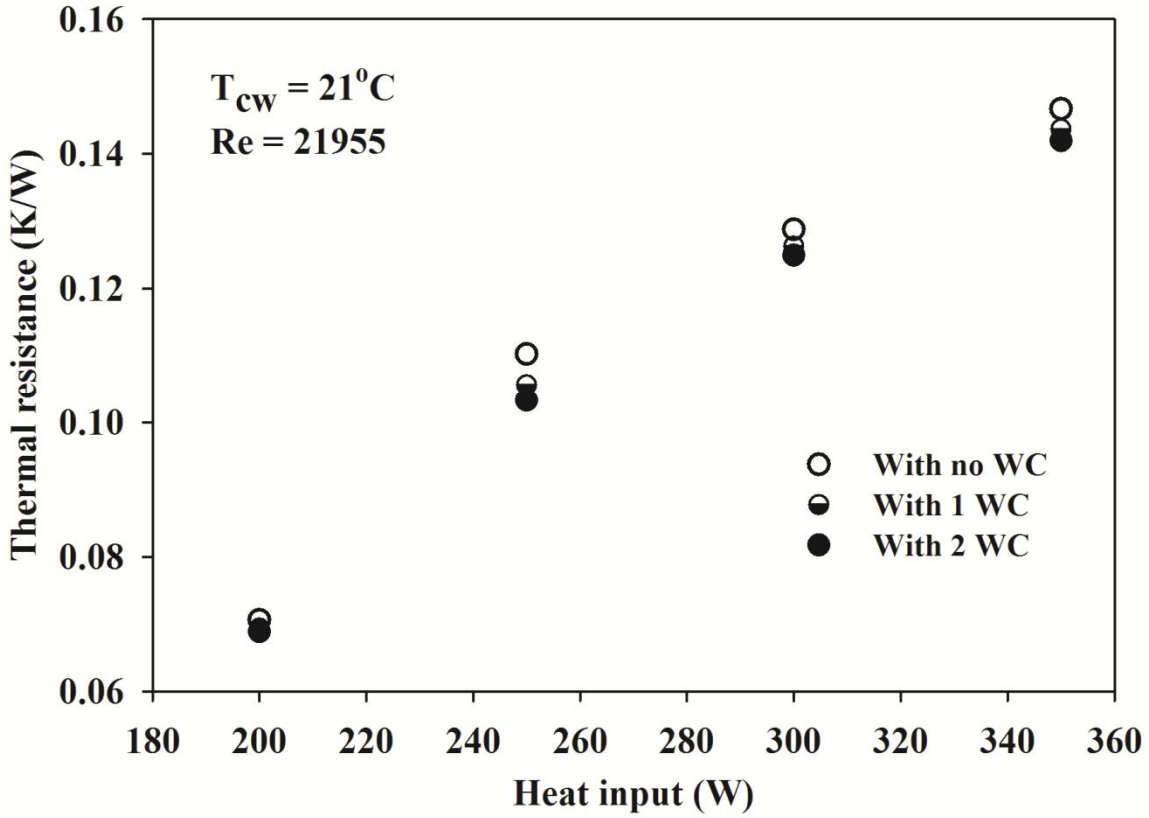

Fig. 6 Effect of heat input on thermal resistance of FHP

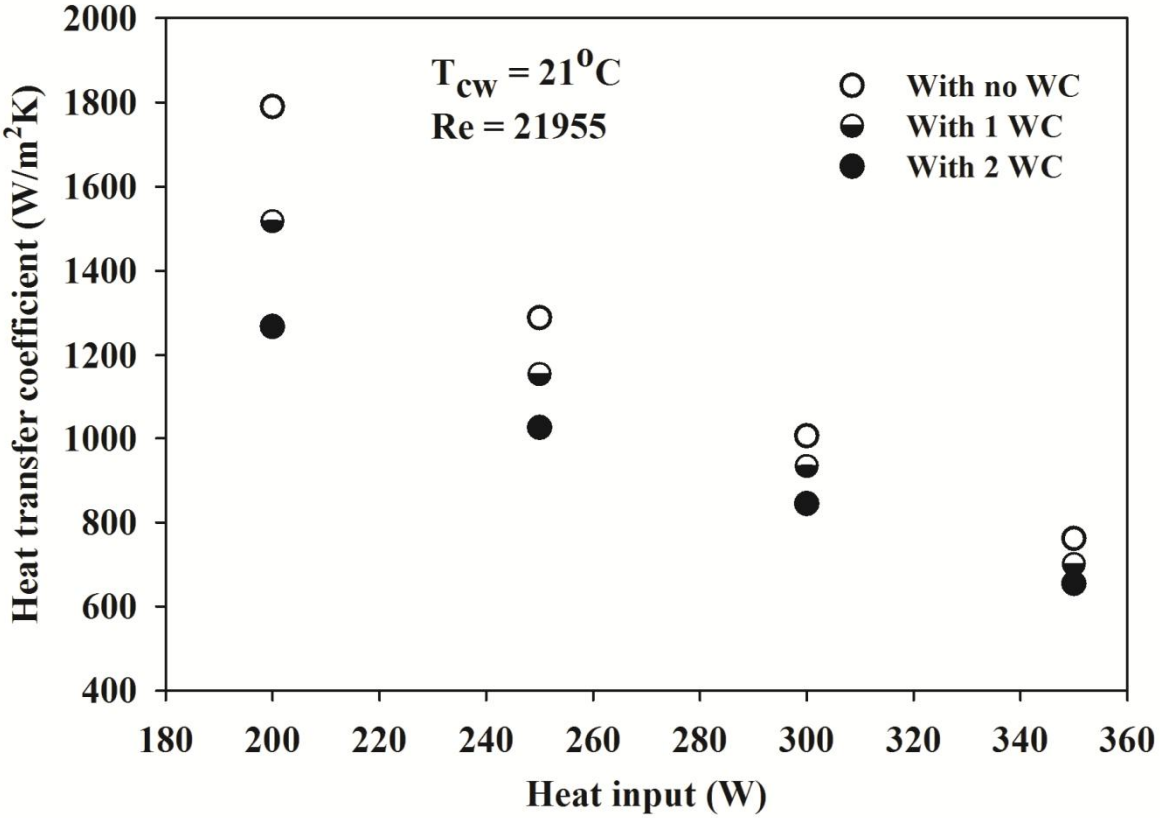

Fig. 7 Effect of heat input on convective heat transfer coefficient of FHP

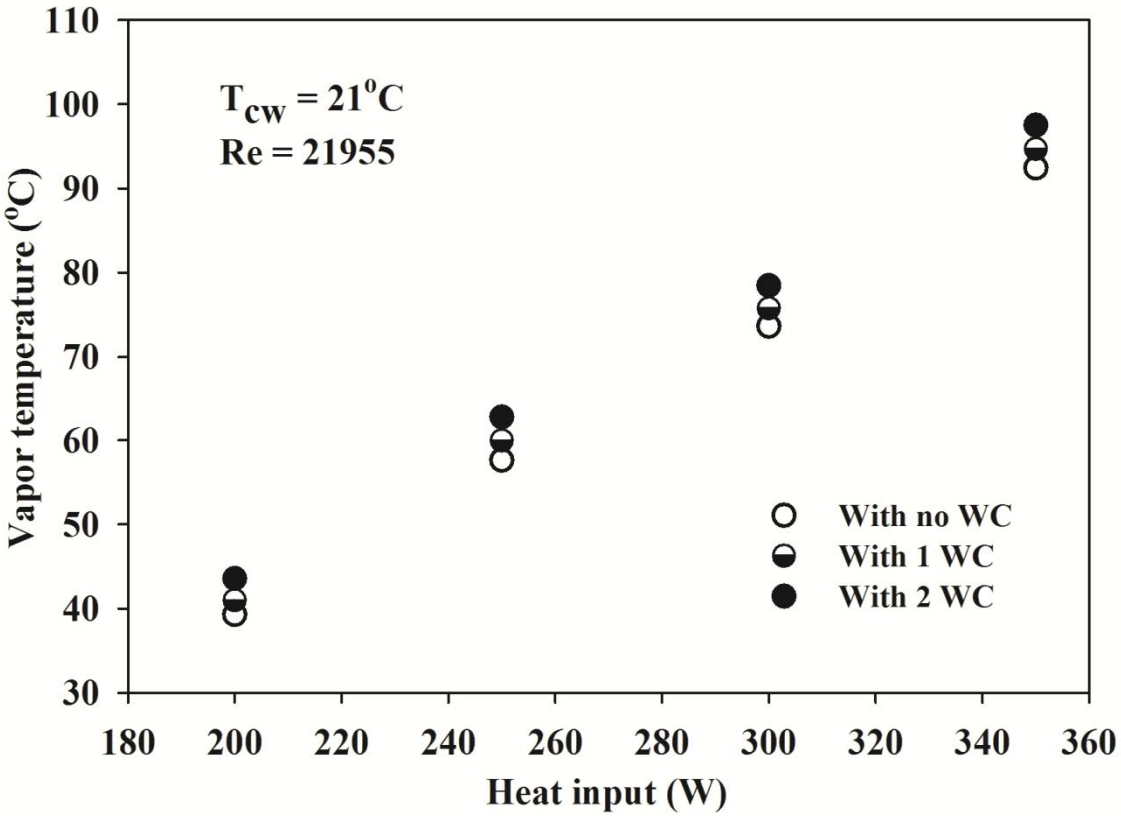

Fig. 8Effect of heat input on vapor temperature of FHP

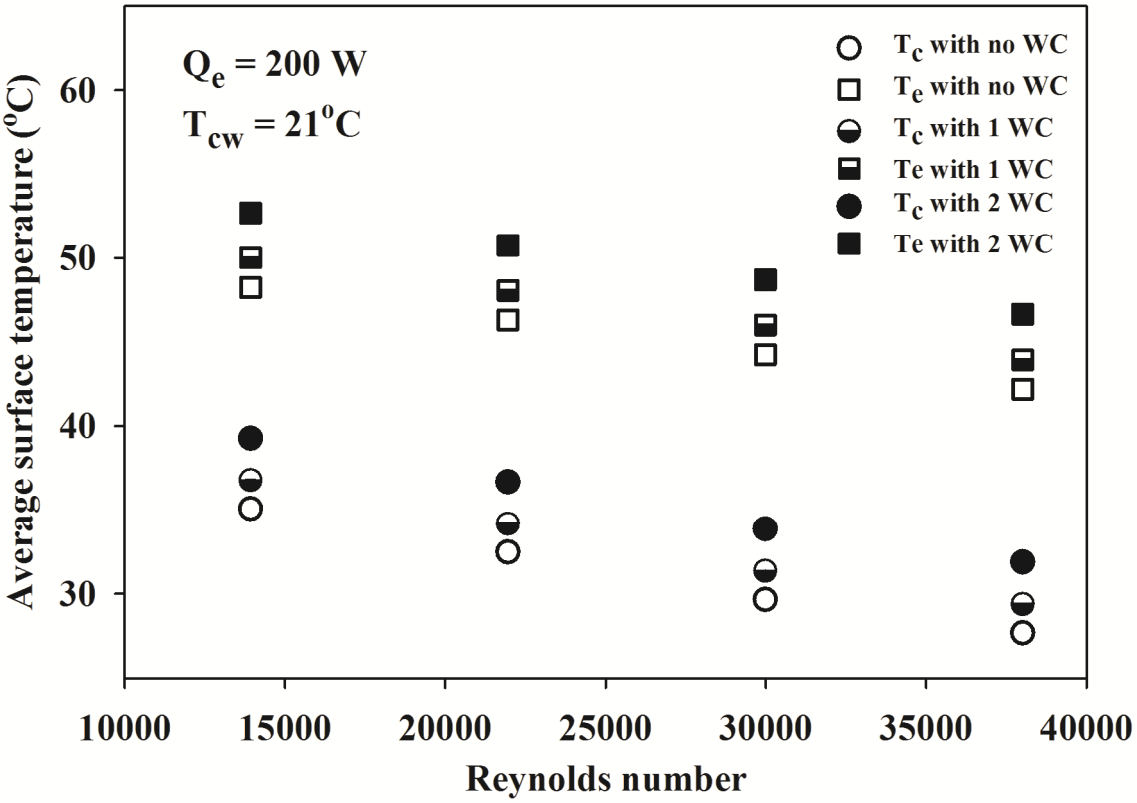

Fig. 9 Effect of Reynolds number of cooling water on the surface temperature of FHP

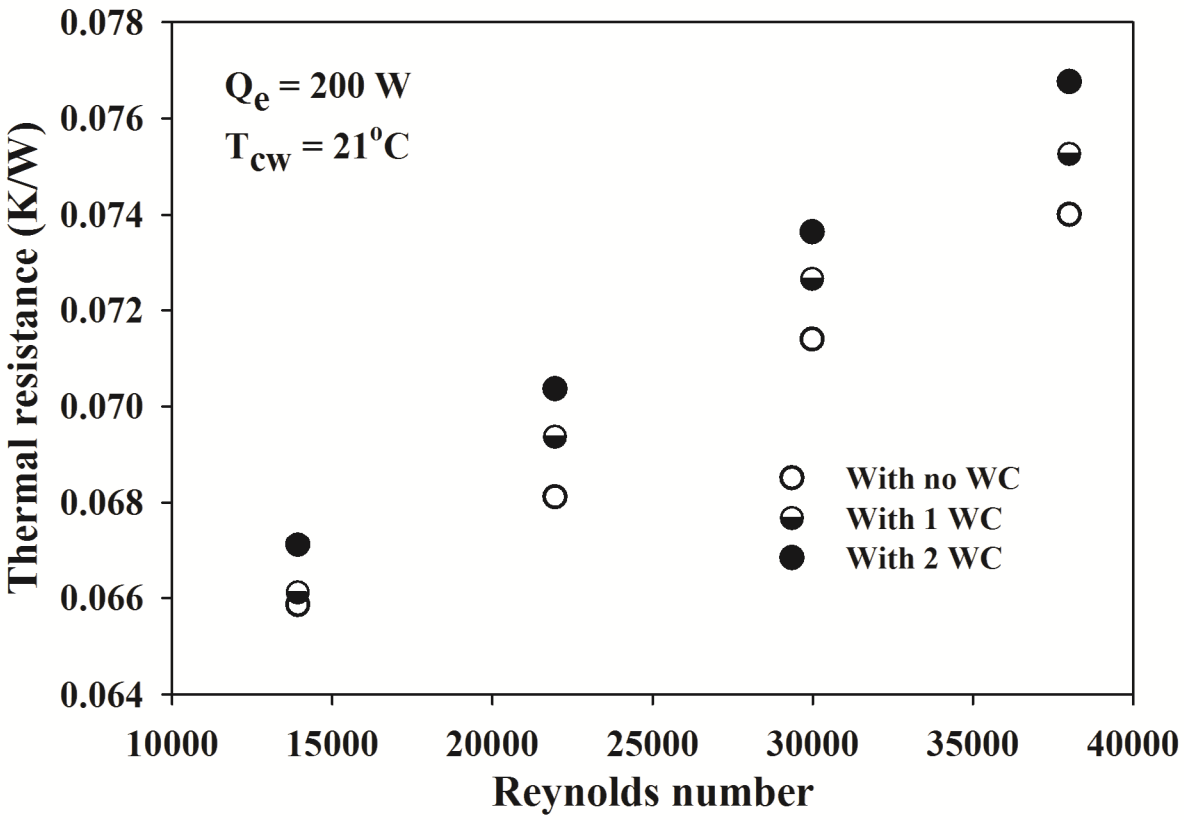

Fig. 10 Effect of Reynolds number of cooling water on thermal resistance of FHP

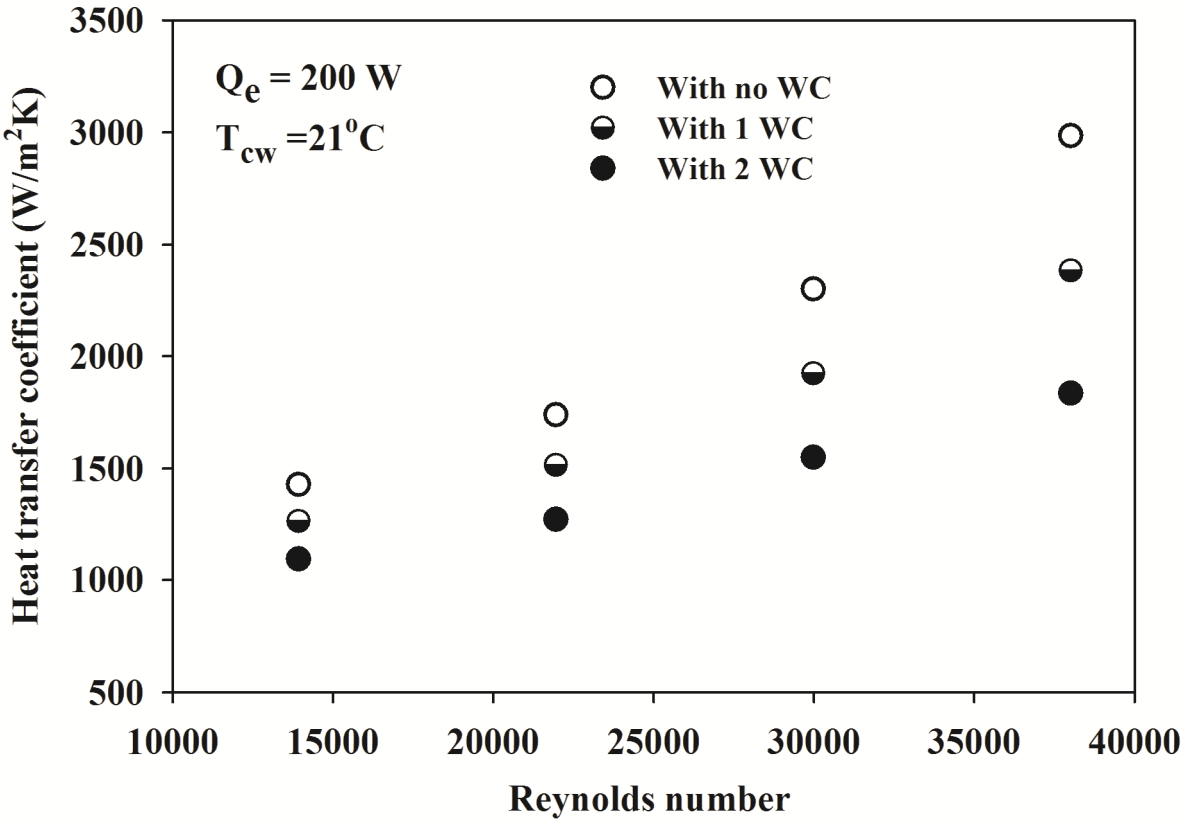

Fig. 11 Effect of Reynolds number of cooling water on the heat transfer coefficient of FHP

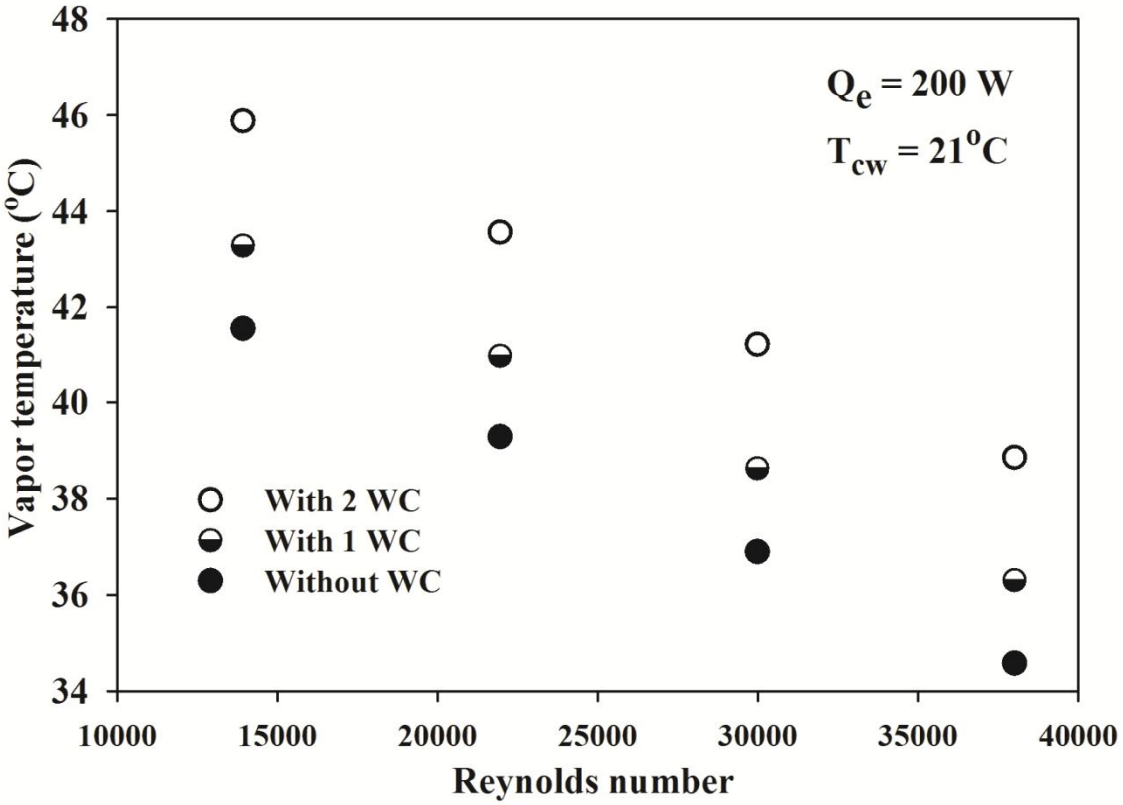

Fig. 12 Effect of Reynolds number of cooling water on vapor temperature of FHP

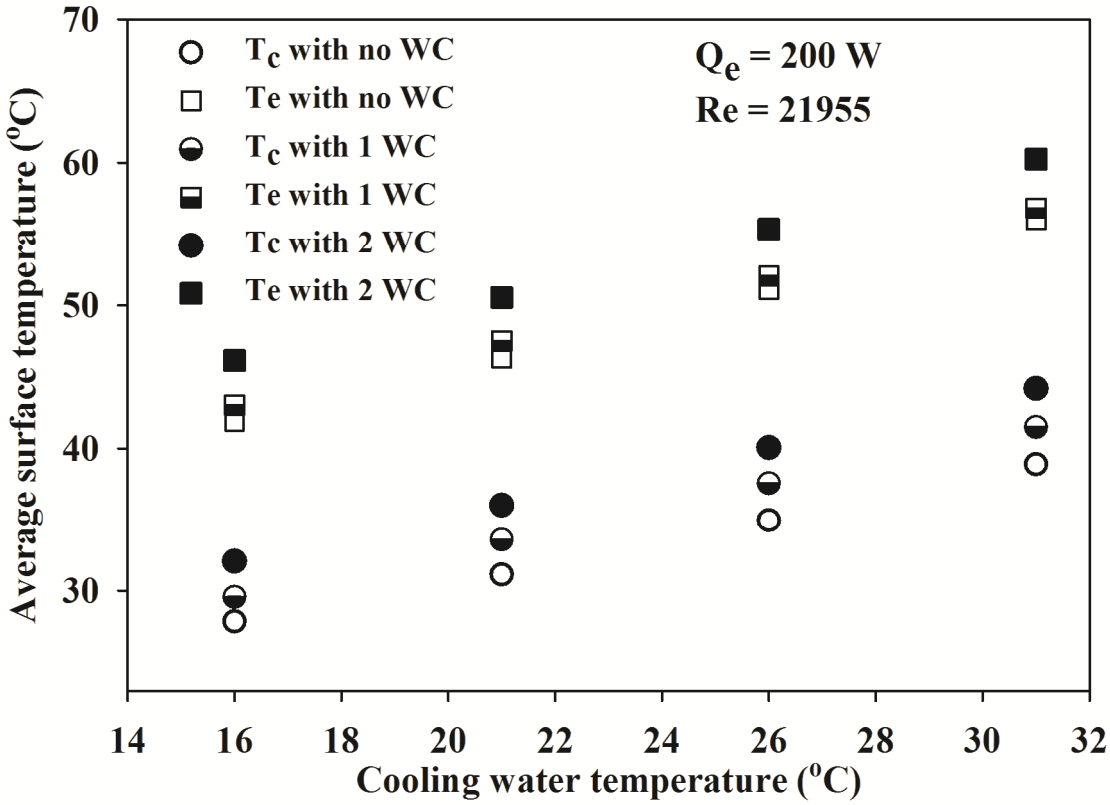

Fig. 13 Effect of cooling water temperature on the surface temperature of FHP

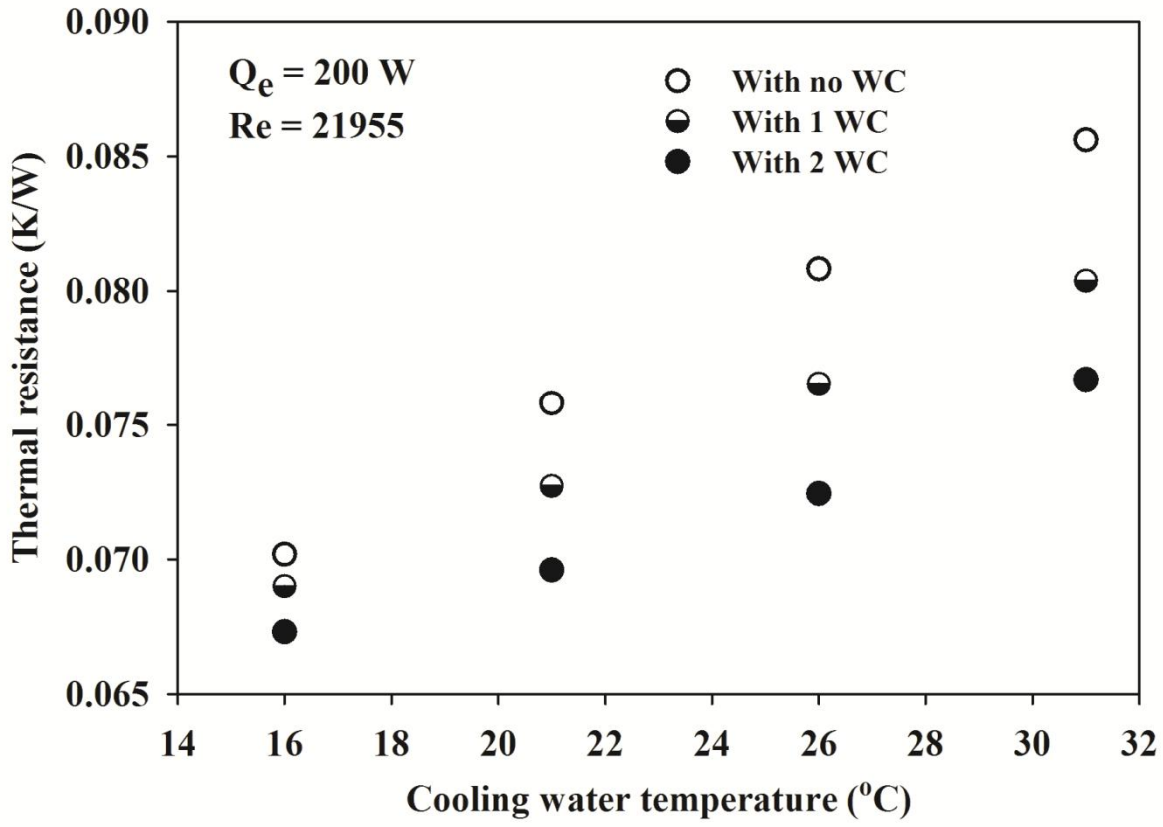

Fig. 14 Effect of cooling water temperature on the thermal resistance of FHP

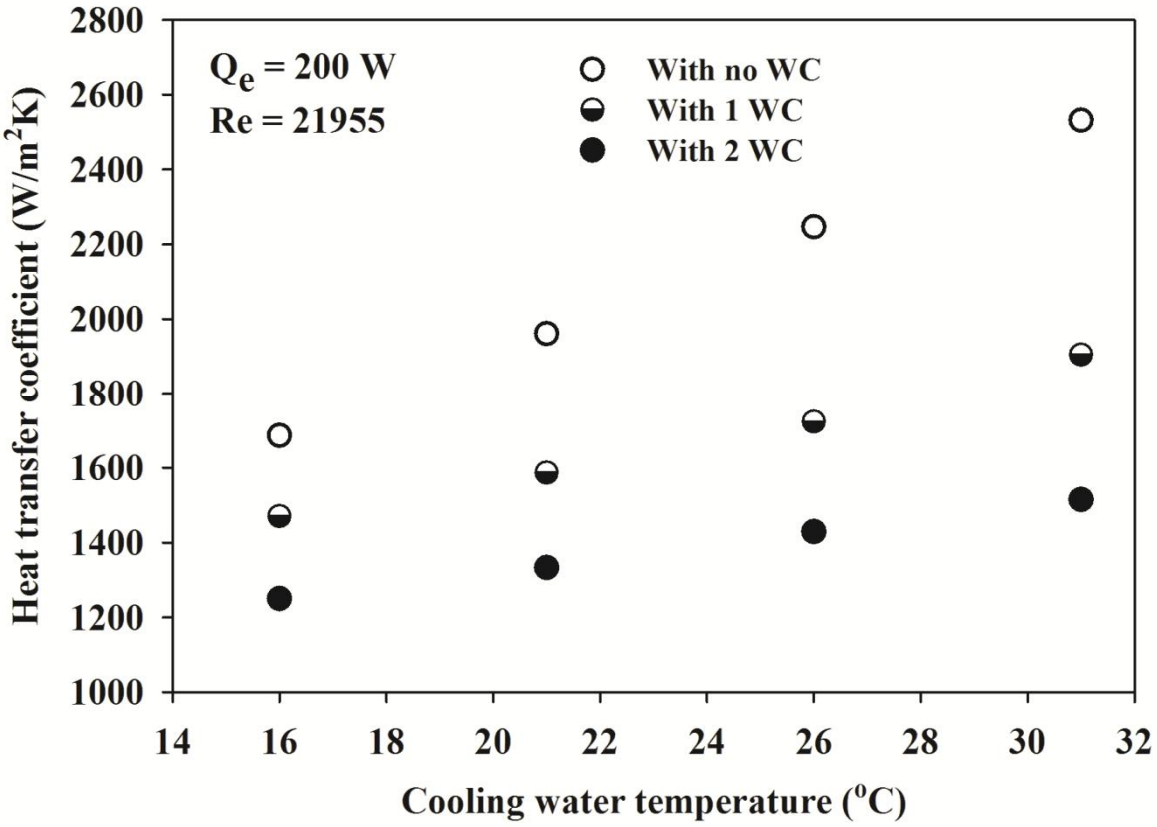

Fig. 15 Effect of cooling water temperature on the heat transfer coefficient of FHP

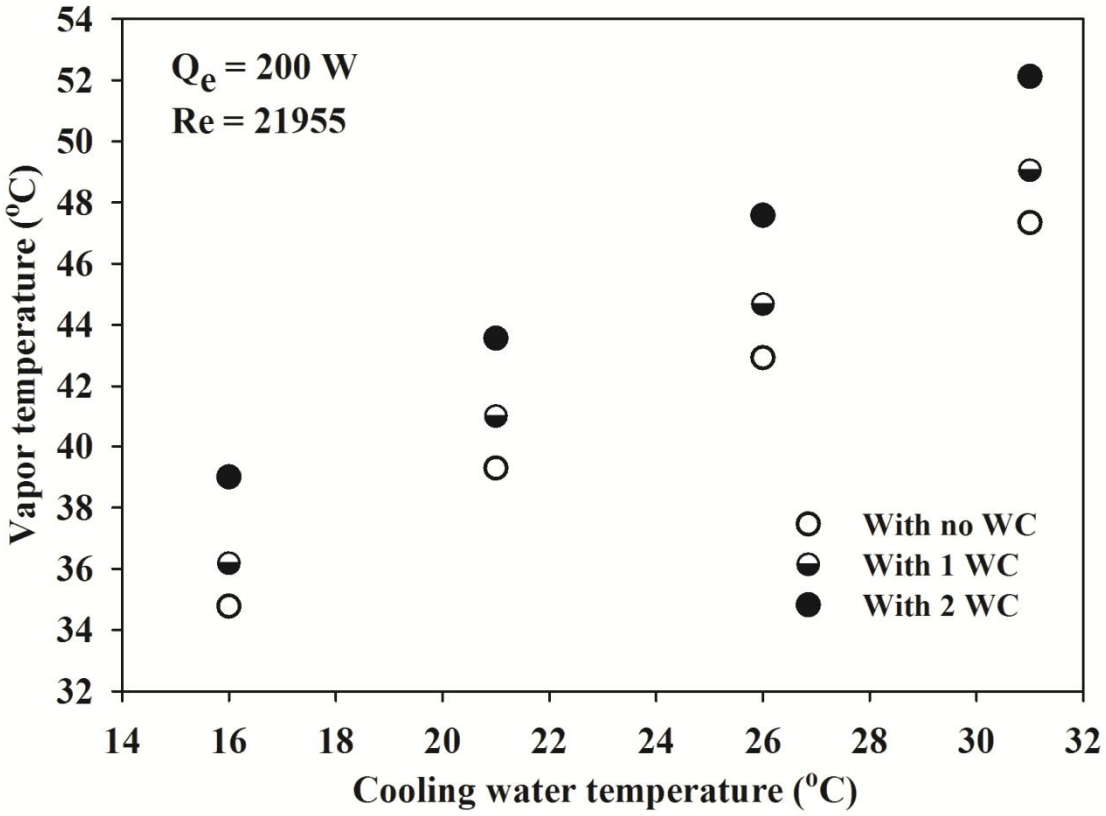

Fig.16 Effect of cooling water temperature on vapor temperature of FHP

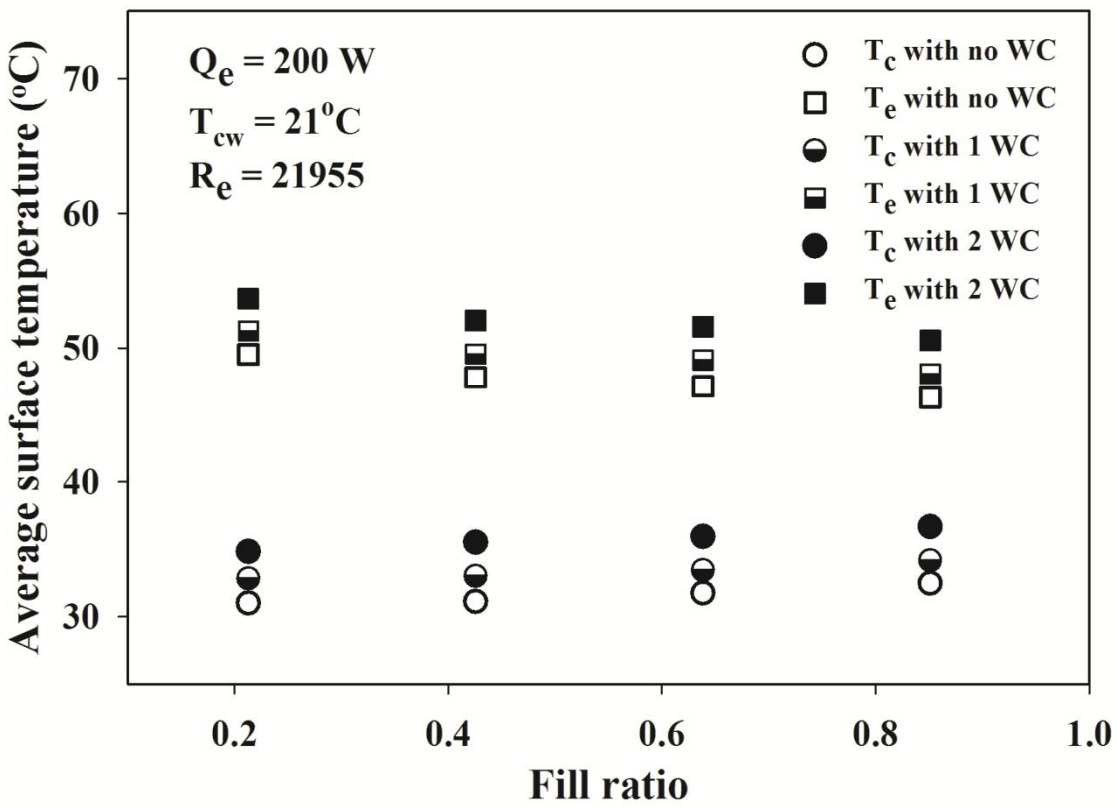

Fig. 17 Effect of fill ratio on the surface temperature of FHP

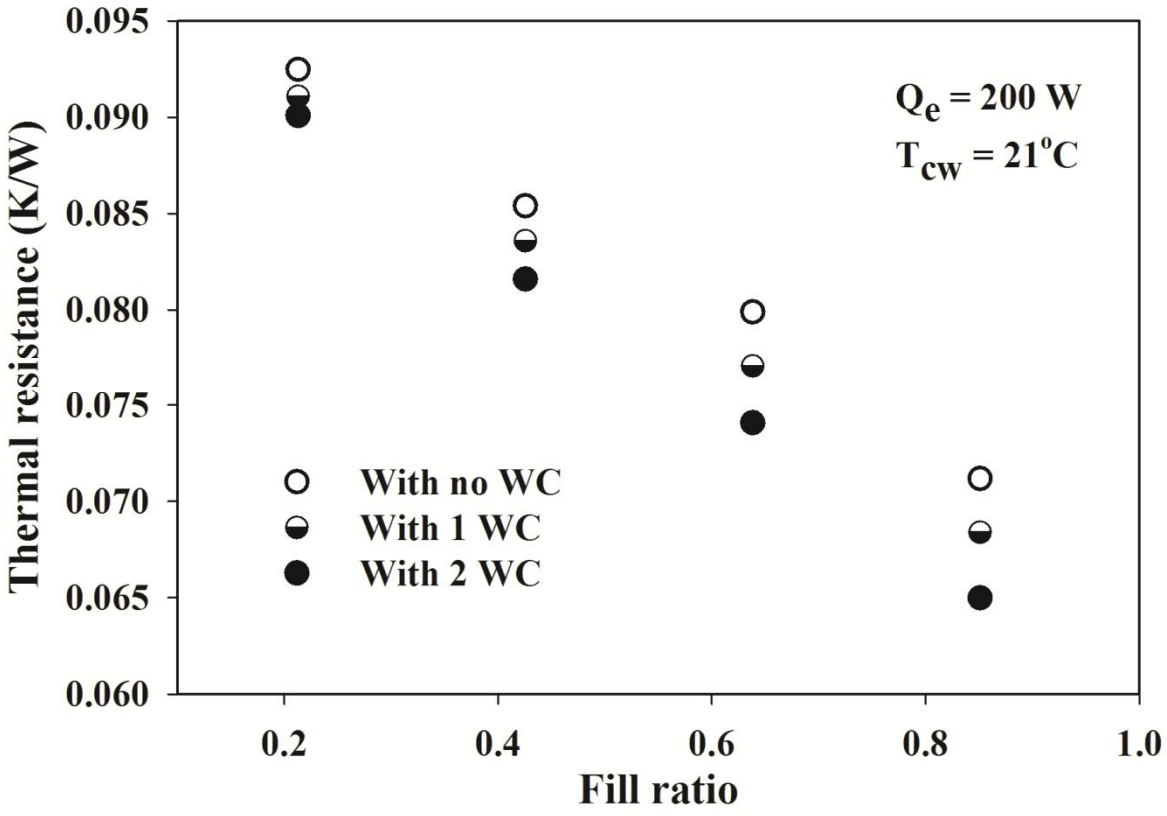

Fig.18 Effect of fill ratio on thermal resistance of FHP

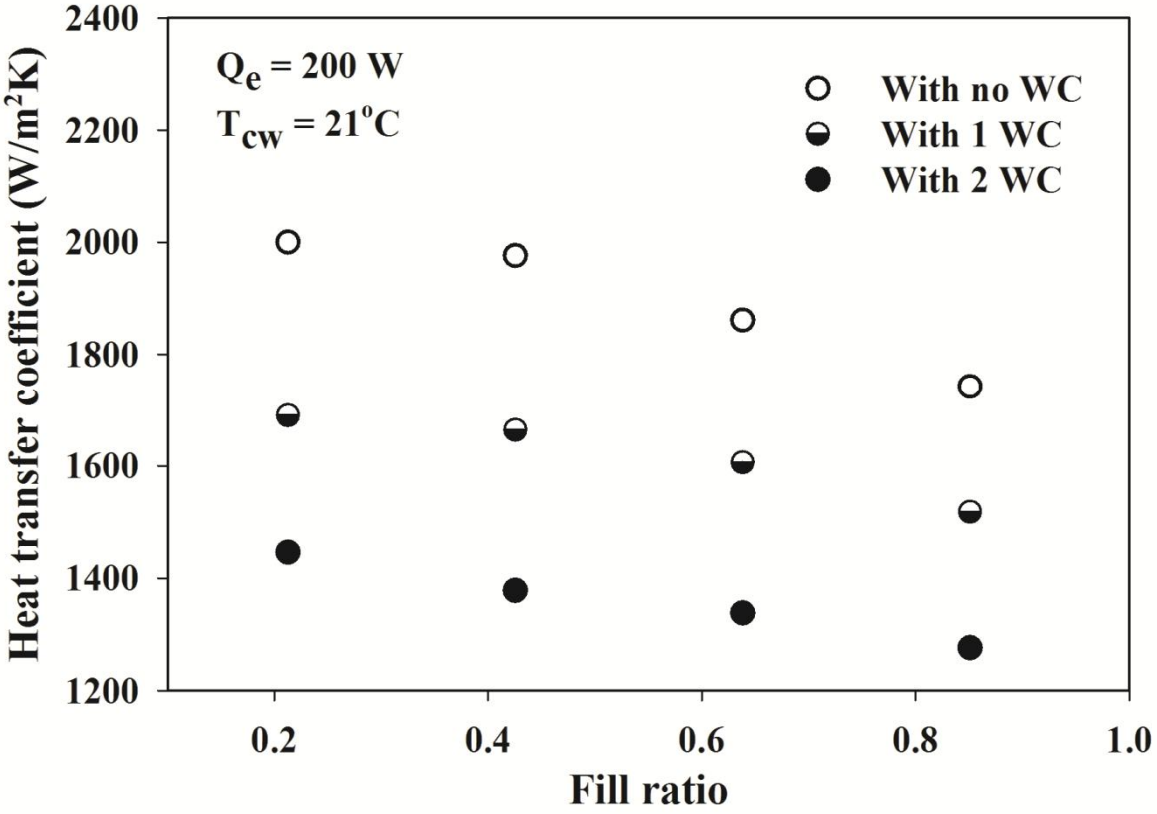

Fig. 19 Effect of fill ratio on the heat transfer coefficient of FHP

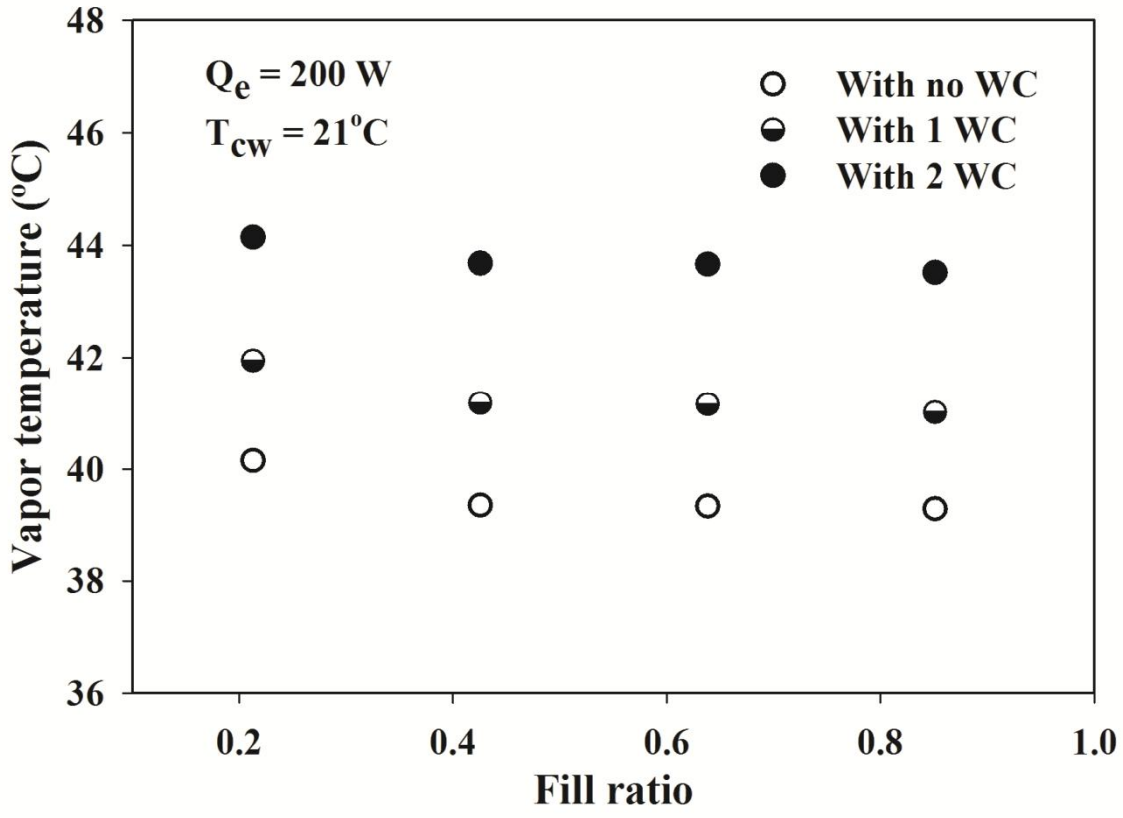

Fig. 20 Effect of fill ratio on vapor temperature of FHP

Highlights

Introduction of wick columns increases the thermal performance of flat heat pipe.

Addition of wick column increases the heat transfer rate and decreases thermal resistance.

Increasing heat input, working fluid charge and cooling water temperature decrease the thermal resistance.

Increasing cooling water flow rate increases the thermal resistance.